



Published in final edited form as:

Arterioscler Thromb Vasc Biol. 2016 May ; 36(5): 984–993. doi:10.1161/ATVBAHA.115.306140.

The Actin-binding Protein Drebrin Inhibits Neointimal Hyperplasia

Jonathan A. Stiber¹, Jiao-Hui Wu¹, Lisheng Zhang¹, Igor Nepliouev¹, Zhu-Shan Zhang¹, Victoria G. Bryson¹, Leigh Brian¹, Rex. C. Bentley², Phillip R. Gordon-Weeks³, Paul B. Rosenberg¹, and Neil J. Freedman¹

¹Department of Medicine, Duke University Medical Center, Durham, NC USA 27710

²Department of Pathology, Duke University Medical Center, Durham, NC 27710

³MRC Centre for Developmental Neurobiology, King's College, London, UK

Abstract

Objective—Vascular smooth muscle cell (SMC) migration is regulated by cytoskeletal remodeling as well as by certain transient receptor potential (TRP) channels, nonselective cation channels that modulate calcium influx. Proper function of multiple TRPC channels requires the scaffolding protein Homer 1, which associates with the actin-binding protein Drebrin. We found that SMC Drebrin expression is upregulated in atherosclerosis and in response to injury and investigated whether Drebrin inhibits SMC activation, either through regulation of TRP channel function via Homer or through a direct effect on the actin cytoskeleton.

Approach and Results—WT and congenic *Dbn*^{-/+} mice were subjected to wire-mediated carotid endothelial denudation. Subsequent neointimal hyperplasia was 2.4 ± 0.3 -fold greater in *Dbn*^{-/+} than in WT mice. Levels of G-actin were equivalent in *Dbn*^{-/+} and WT SMCs, but there was a 2.4 ± 0.5 -fold decrease in F-actin in *Dbn*^{-/+} SMCs compared with WT. F-actin was restored to WT levels in *Dbn*^{-/+} SMCs by adenoviral-mediated rescue expression of Drebrin. Compared with WT SMCs, *Dbn*^{-/+} SMCs exhibited increased TRP channel activity in response to platelet-derived growth factor, increased migration assessed in Boyden chambers, and increased proliferation. Enhanced TRP channel activity and migration in *Dbn*^{-/+} SMCs were normalized to WT levels by rescue expression of not only WT Drebrin but also a mutant Drebrin isoform that binds actin but fails to bind Homer.

Conclusions—Drebrin reduces SMC activation through its interaction with the actin cytoskeleton but independently of its interaction with Homer scaffolds.

Keywords

Drebrin; homer; actin; smooth muscle; neointimal hyperplasia

For Correspondence: Jonathan A. Stiber, Box 103032, Duke University Medical Center, Durham, NC 27710, Phone: 919-684-1146, Fax: 919-613-5145, stibe001@mc.duke.edu.

Disclosures
None.

Introduction

Drebrin, developmentally regulated brain protein, was first identified by proteomic techniques from the brain of the developing chick.¹ Drebrin has been shown to stabilize actin filaments through direct binding and to link the actin cytoskeleton to the microtubular network.^{2,3} The N-terminal half of Drebrin contains two domains that bind filamentous actin (F-actin): a helical domain, which binds F-actin tonically, and a coiled-coil domain, which binds actin only when it is phosphorylated by Cdk5 (on Ser142); cooperative binding of F-actin by these 2 domains enables Drebrin to bundle actin.^{3,4} In mammals a single Drebrin gene (*Dbn1*) transcript undergoes alternative splicing to produce two isoforms: adult (Drebrin A) and embryonic (Drebrin E).⁵ Drebrin A in neurons mediates reorganization of actin filaments and thereby contributes to memory.^{6,7} Drebrin knockout mice were recently reported to exhibit decreased dendritic spine density, neurotransmitter receptor levels, and memory-related synaptic plasticity in hippocampal neurons when compared to WT mice.⁸ Outside of the nervous system, Drebrin E expression has been reported in a variety of cell types.⁹⁻¹¹

Drebrin has also been identified by proteomic analysis as part of a protein complex associated with transient receptor potential (TRP) channels,¹² a family of nonselective cation channels that mediate calcium influx in SMCs and have been implicated in the regulation of vascular remodeling.¹³⁻¹⁵ Multiple members of the TRPC subfamily of TRP channels have been shown to require the scaffolding protein Homer 1 for proper function^{16,17} and several groups have shown that Homer scaffolds associate with Drebrin through an interaction mediated by two Homer-binding sites within the Drebrin C-terminal domain.¹⁸⁻²⁰ We made the unexpected observation that Drebrin is abundantly expressed in SMCs and is upregulated in response to arterial injury. Because neointimal hyperplasia, a process which involves both SMC migration and proliferation, may involve SMC TRP channels¹⁵ and because TRPC channel function is regulated by the Drebrin-binding protein Homer,¹⁶ we tested whether Drebrin affects SMC proliferation and migration through its interaction with Homer and/or F-actin.

Materials and Methods

Materials and Methods are available in the online-only Data Supplement.

Results

Drebrin is Expressed Abundantly in SMCs

Because we sought to determine the function of Drebrin outside the CNS, in vascular tissue, we created a Drebrin knockout mouse model on a pure C57BL/6 background that prevented expression of both the A and the E isoforms of Drebrin. The *Dbn* knockout strategy employed by the NIH Knockout Mouse Project tagged the Drebrin gene with a LacZ reporter that created a constitutive null mutation in *Dbn*—because efficient splicing to the lacZ reporter results in truncation of the endogenous transcript (Figure 1A). *Dbn*^{-/+} mice were phenotypically indistinguishable from WT mice, and their *Dbn*^{-/-} progeny lacked any Drebrin protein as demonstrated by immunoblotting (Figure 1B). Although *Dbn*^{-/-} mice

generated on a mixed genetic background were not reported to exhibit neonatal lethality,⁸ our *Dbn*^{-/-} mice on a C57BL/6 genetic background exhibited neonatal lethality for unclear reasons (Table 1). No gross anatomic defects were noted on necropsy. Histologic sections of WT and *Dbn*^{-/-} aortas showed equivalent lumen areas and wall areas (Figure I A-B in the online-only Data Supplement). No heart defects were noted in *Dbn*^{-/-} neonates (Figure I C in the online-only Data Supplement).

In *Dbn*^{+/-} mice, the *Dbn* trapping cassette enabled the endogenous Drebrin promoter to drive expression of β -galactosidase independently of the N-terminal domain of Drebrin (because of the IRES segment, Figure 1A). Thus, β -galactosidase activity in *Dbn*^{+/-} mice served as a read-out for relative Drebrin expression in various tissues. As expected based on previous work,²¹ *Dbn*^{+/-} mice showed the highest β -galactosidase activity levels in the brain. However, Drebrin gene expression—and thus β -galactosidase activity—was also very high in vascular tissue (Figure 1C-D). With one or two copies of the β -galactosidase reporter gene, respectively, *Dbn*^{+/-} and *Dbn*^{-/-} aortas demonstrated high levels of β -galactosidase activity in medial smooth muscle cells (SMCs) (Figure 1D). Immunoblotting also demonstrated that whereas Drebrin expression is abundant in mouse primary SMCs, it is not detectable in mouse primary endothelial cells or macrophages, or in mouse T cell lymphoma (RMA) cells (Figure 1E). *Dbn*^{+/-} SMCs expressed ~50% the amount of Drebrin protein as WT SMCs (Figure 1F).

Drebrin Upregulates with Atherosclerosis and Endothelial Injury

The abundant expression of Drebrin in vascular SMCs raised the possibility that Drebrin may be involved in arterial pathologies, just like the TRPC1 channel¹⁵ which, like Drebrin, also binds Homer.¹⁶ Accordingly, we examined whether Drebrin expression is upregulated in atherosclerosis. Human peroneal arteries from surgically amputated legs were separated into segments that demonstrated (a) various degrees of atherosclerosis (Figure 2A and Figure II of the online-only Data Supplement), or (b) minimal or no atherosclerosis (Figure 2A). Although medial SM α -actin immunofluorescence was equivalent in atherosclerotic and non-atherosclerotic arterial segments, medial Drebrin immunofluorescence was 3.0 ± 0.5 -fold greater in atherosclerotic, as compared with non-atherosclerotic segments (Figure 2A-B). Similar findings were obtained in *ApoE*^{-/-} mice: medial Drebrin immunofluorescence was 4 ± 1 -fold greater in atherosclerotic, as compared with non-atherosclerotic brachiocephalic arteries (Figure III of the online-only Data Supplement). Thus, SMC Drebrin appeared to be upregulated in atherosclerotic arteries of humans and mice.

To determine whether arterial injury also upregulates SMC Drebrin in the mouse, we denuded the endothelium of common carotid arteries in WT mice.^{22,23} This procedure produces neointimal hyperplasia that comprises SMCs from only the artery itself (and not from bone marrow progenitor cells), as we have shown with GFP-transgenic bone marrow transplantation.²³ Drebrin upregulated 3.8 ± 0.6 -fold in medial and neointimal SMCs of injured arteries, as compared with uninjured arteries, even though SM α -actin levels remained equivalent (on a per-cell basis) in both injured and uninjured arteries (Figure 2C-D). To corroborate this finding, we assayed in injured *Dbn*^{+/-} mouse carotids the extent of β -

galactosidase expression—which is proportional to Drebrin expression because it is driven by the Drebrin promoter upstream of the Drebrin trapping cassette (Figure 1). In endothelium-denuded *Dbn*^{-/+} carotids, β -galactosidase upregulated 1.5 ± 0.1 -fold (Figure IV A-B of the online-only Data Supplement). Thus, assayed as the expression of either Drebrin protein or as Drebrin promoter-driven β -galactosidase protein, mouse SMC Drebrin upregulated with arterial injury.

Drebrin Haploinsufficiency Augments Neointimal Hyperplasia and Vascular Remodeling

Because SMC Drebrin was upregulated in response to arterial injury, it seemed plausible that SMC Drebrin affects vascular remodeling. To test this possibility, we compared the responses of WT and congenic *Dbn*^{-/+} mice to carotid endothelial denudation.^{22,23} Prior to endothelial denudation, *Dbn*^{-/+} and WT carotids were indistinguishable with regard to luminal and medial areas. However, 4 weeks after endothelial denudation, *Dbn*^{-/+} carotids exhibited 2.4 ± 0.3 -fold more neointimal area, 1.6 ± 0.3 -fold greater medial area, and 2.0 ± 0.4 -fold greater total arterial cross-sectional area (reflecting greater outward arterial remodeling) than WT carotids (Figure 3 A-B). That the neointimal hyperplasia comprised only SMCs, and not macrophages, was demonstrated by staining for (a) SM α -actin (Figure 2C) and SM-MHC and (b) CD11b, respectively (Figure V A-C of the online-only Data Supplement). Furthermore, augmentation of neointimal hyperplasia by Drebrin deficiency appeared to involve SMC hyperplasia, as demonstrated by medial SMC nuclear density—which was greater in *Dbn*^{-/+} than in WT mice (Figure V F of the online-only Data Supplement). Injured *Dbn*^{-/+} carotids demonstrated only ~60% of the Drebrin protein levels observed in injured WT carotids (Figure VI A-B in the online-only Data Supplement). Thus, Drebrin activity appeared to reduce neointimal hyperplasia.

Drebrin Stabilizes Actin Filaments in SMCs

Because neointimal hyperplasia fundamentally involves SMC proliferation and migration,^{22,23} and because cytoskeletal rearrangement is fundamental to cell migration, we tested the role of Drebrin in SMC actin dynamics. By confocal microscopy, endogenous Drebrin immunofluorescence co-localized with phalloidin-stained actin filaments (Figure 4A) and with SM α -actin filaments (Figure VII A in the online-only Data Supplement). Thus, Drebrin appeared to interact with F-actin in intact SMCs. To determine whether Drebrin affects actin stability in SMCs, we quantitated F-actin in proliferating *Dbn*^{-/+} and WT SMCs after separating F-actin from globular actin (G-actin) by ultracentrifugation. *Dbn*^{-/+} SMCs contained ~2-fold less F-actin than WT SMCs—assessed by immunoblotting either for β -actin (Figure 4B-C) or SM α -actin (Figure VII B, C in the online-only Data Supplement). Despite observing decreased F-actin levels in *Dbn*^{-/+} SMCs, we detected no increase in G-actin levels in *Dbn*^{-/+} (as compared with WT) SMCs (Figures 4 and VII). This apparent paradox may be explained by considering that, in our disrupted SMC assays, F-actin represented only ~10% of total actin. Consequently, the ~2-fold decrease in F-actin seen in *Dbn*^{-/+} SMC lysates would correspond to only a ~5% increase in the G-actin fraction—an increment that was below the limit of our assay sensitivity. Thus, Drebrin appeared to stabilize F-actin in SMCs as it does in neurons.⁴

To confirm that reduced actin stabilization in *Dbn*^{-/+} SMCs could be attributed to Drebrin deficiency itself, we assessed F-actin levels in *Dbn*^{-/+} SMCs after rescuing Drebrin expression by adenoviral transduction. WT and *Dbn*^{-/+} SMCs were infected with recombinant adenoviruses encoding either β -galactosidase or Drebrin, and then were subjected to actin fractionation by ultracentrifugation. β -galactosidase-transduced *Dbn*^{-/+} SMCs still demonstrated 2.2 ± 0.3 -fold less F-actin than β -galactosidase-transduced WT SMCs. However, re-expression of Drebrin in *Dbn*^{-/+} SMCs restored F-actin levels to those seen in WT SMCs. (Figure 4D-E).

Loss of Drebrin Results in Increased TRP Channel Activity

Could augmentation of neointimal hyperplasia in *Dbn*^{-/+} mice involve the interaction between Drebrin and Homer, perhaps because of effects on TRP channel activity? TRP channel activity has been shown to promote SMC migration,^{15,24} and Homer scaffolds regulate TRP channel activity.¹⁶ Accordingly, we compared *Dbn*^{-/+} and WT SMCs for TRP channel current density using the whole-cell patch clamp approaches we previously described.¹⁷ *Dbn*^{-/+} SMCs demonstrated 1.8 ± 0.4 -fold greater inward current density than WT SMCs under basal conditions and 1.7 ± 0.3 -fold greater inward current density after stimulation with 1 nmol/L PDGF (Figure 5A-C). Currents were blocked by 10 μ mol/L GdCl₃, as would be expected for a TRP channel current.²⁵ Thus, Drebrin appears to constrain TRP channel activity in SMCs as Homer1 does in skeletal muscle myocytes.¹⁷ In contrast, we found equivalent store-operated currents in WT and *Dbn*^{-/+} SMCs (Figure VIII in the online-only Data Supplement)-even though SMC migration and proliferation can be regulated by store-operated calcium influx,^{26,27} which is mediated by Orai channels that are activated by STIM1 in response to internal calcium store depletion.^{26,27} Thus, the effect of Drebrin on PDGF-stimulated calcium influx appeared to be TRP channel-specific.

To ascertain whether the enhanced TRP channel activity in *Dbn*^{-/+} SMCs could be attributed to Drebrin deficiency, we transduced *Dbn*^{-/+} SMCs with our adenoviruses encoding β -galactosidase or Drebrin. Adenoviral transduction itself did not alter the increased TRP channel activity observed in *Dbn*^{-/+} SMCs compared with WT SMCs: β -galactosidase-transduced *Dbn*^{-/+} SMCs showed 2.8 ± 0.5 -fold greater TRP channel activity than β -galactosidase-transduced WT SMCs in the basal state, and 1.8 ± 0.2 -fold greater TRP channel activity in the PDGF-stimulated state (Figure 5D). However, rescue expression of WT Drebrin levels in *Dbn*^{-/+} SMCs reduced PDGF-activated TRP activity to levels observed in WT SMCs (Figure 5D). Thus, Drebrin deficiency in *Dbn*^{-/+} SMCs was responsible for increased TRP channel activity. To determine whether Drebrin reduces TRP channel activity by binding to Homer or by binding to F-actin, we performed our Drebrin rescue in *Dbn*^{-/+} SMCs with a Drebrin mutant that cannot bind Homer but nonetheless does bind F-actin: Drebrin(F543A, F621A).¹⁸ Just like WT Drebrin, Drebrin(F543A/F621A) restored TRP channel activity in *Dbn*^{-/+} SMCs to WT levels (Figure 5D). Thus, Drebrin inhibits TRP channel activity independently of its interaction with Homer, likely through its effect on cytoskeletal organization.

Drebrin Deficiency Increases SMC Migration and Proliferation

Because Drebrin regulated TRP channel activity independently of its association with Homer, we reasoned that Drebrin could also regulate SMC migration independently of a Drebrin/Homer interaction. To test this possibility, we first examined the migration of SMCs from *Dbn*^{-/+} and WT littermate mice.²² Migration of *Dbn*^{-/+} and WT SMCs were equivalent in the absence of agonist (Figure 6A). However, in response to PDGF, *Dbn*^{-/+} SMCs migrated 56 ± 2% faster than WT SMCs (*p* < 0.05, Figure 6A). Importantly, WT and *Dbn*^{-/+} SMCs demonstrated equivalent levels of PDGF receptor-β expression, equivalent extents of PDGF-promoted PDGF receptor-β activation (assessed by autophosphorylation), and equivalent extents of PDGF-induced signaling through the phosphoinositide 3-kinase pathway, as exemplified by phosphorylation of Akt (Figure 6B-C). Thus, although Drebrin did not affect SMC signaling in response to PDGF, it suppressed SMC migration in response to PDGF—a finding consistent with the ability of Drebrin to reduce neointimal hyperplasia (Figure 3).

In Figure 5, we found that PDGF evoked greater TRP channel current density in *Dbn*^{-/+} than in WT SMCs, and that these PDGF-induced currents were blocked by 10 μM Gd³⁺ in our external solution for patch clamp studies. Could Drebrin-mediated inhibition of SMC TRP channel currents underlie Drebrin's inhibition of SMC migration? To address this question, we first used fluorescent Ca²⁺ imaging to confirm that 10 μmol/L Gd³⁺ inhibited PDGF-evoked Ca²⁺ influx in migration medium just as it inhibited TRP channel currents in external buffer solution used for patch clamp studies (Figure IX in the online-only Data Supplement). We then assessed the effect of Gd³⁺ on SMC migration. However, we found no effect of 10 μmol/L Gd³⁺ on basal or PDGF-evoked migration, in either WT or *Dbn*^{-/+} SMCs (Figure 6C). Indeed, either in the absence or presence of Gd³⁺, *Dbn*^{-/+} SMCs migrated ~60% faster than WT SMCs. Thus, Drebrin appears to regulate SMC migration independently of its effects on TRP channel activity.

Because Drebrin regulated SMC migration independently of its ability to regulate TRP channels, we asked whether Drebrin regulates SMC migration independently of its interaction with the TRP channel-binding protein Homer. To address this question, we rescued Drebrin expression in *Dbn*^{-/+} SMCs with either (a) WT Drebrin or (b) the F543A/F621A mutant Drebrin that cannot bind Homer but that can bind F-actin normally, just as we did in Figure 5. When SMCs were transduced with control (β-galactosidase-encoding) adenovirus, PDGF evoked more migration from *Dbn*^{-/+} than from WT SMCs (Figure 6D); thus, adenoviral transduction itself did not alter the Drebrin-mediated suppression of SMC migration observed in Figure 6A. However, when SMCs were transduced with adenovirus encoding either WT Drebrin or Drebrin(F543A/F621A), PDGF evoked equivalent migration in *Dbn*^{-/+} and WT SMCs (Figure 6D). Thus, we can infer that the hypermigratory phenotype of *Dbn*^{-/+} SMCs results just from deficiency of Drebrin—not only because *Dbn*^{-/+} SMC migration is normalized by rescue expression of Drebrin, but also because the hypermigratory phenotype of *Dbn*^{-/+} SMCs manifested in comparisons of 5 independently isolated *Dbn*^{-/+} and WT SMC lines (Figure 6). Furthermore, because the WT migratory phenotype was rescued in *Dbn*^{-/+} SMCs by re-expression of Drebrin that either lacks or

retains Homer-binding ability, it appears that Drebrin regulates SMC migration through mechanisms independent of Homer.

Neointimal hyperplasia involves not only SMC migration but also SMC proliferation.²² Accordingly, because Drebrin reduced neointimal hyperplasia (Figure 3), we asked whether Drebrin reduces SMC proliferation as it reduced SMC migration. To address this question, we compared the proliferative responses of *Dbn*^{-/+} and WT SMCs to 10% fetal bovine serum (Figure 6E). The growth curves diverged after only 2 days; after 9 days, *Dbn*^{-/+} SMCs proliferated $41 \pm 5\%$ more than WT SMCs. Congruently, PDGF induced ~40% more thymidine incorporation in *Dbn*^{-/+} than in WT SMCs, and this difference was eliminated by rescue of Drebrin expression in *Dbn*^{-/+} SMCs (Figure X of the online-only Data Supplement). Data in mice also supported the inference that Drebrin deficiency promotes SMC proliferation: proliferating cell nuclear antigen (PCNA) –positive SMCs were more prevalent in injured carotids from *Dbn*^{-/+} than from WT mice, and the SMC nuclear density of the carotid media was greater in *Dbn*^{-/+} than in WT mice (Figure V of the online-only Data Supplement).

Discussion

This work provides the first evidence that Drebrin is abundantly expressed in vascular SMCs and that Drebrin plays a critical function in SMC migration and proliferation, both *in vitro* and *in vivo*. We further found that Drebrin regulates SMC migration through its actin-stabilizing, rather than its Homer-binding activity. Although other studies have also demonstrated Drebrin-mediated actin stabilization using electron and atomic force microscopy^{4,28,29} as well as intact-cell assays,^{4,30,31} our data provide the first evidence that Drebrin stabilization of actin filaments plays a regulatory role in vascular remodeling in response to injury.

That Drebrin may inhibit SMC migration through its effect on cytoskeletal organization is consistent with the effects on cell migration of other actin-binding proteins. For example, loss of the F-actin-stabilizing protein Abp1 increases the invasive migration of transformed fibroblasts.³² Even though Drebrin-mediated stabilization of F-actin may, by itself, explain Drebrin-mediated inhibition of SMC migration,^{4,29} it is also possible that Drebrin regulates migration indirectly, by effects of Drebrin on other actin-binding proteins (Figure XI of the online-only Data Supplement). For example, increased activity of the F-actin-severing protein cofilin promotes migration of prostate cancer cells.³³ Because Drebrin competes with cofilin for binding to F-actin,³⁴ Drebrin activity may decrease cofilin-mediated actin depolymerization and thus decrease SMC migration. Drebrin's effects on actin organization may also affect SMC migration and proliferation indirectly through changes in gene expression regulated by myocardin and myocardin-related transcription factors (MRTFs), which are regulated by actin dynamics.³⁵ Enhanced actin polymerization drives nuclear translocation of MRTFs and promotes serum response factor-mediated gene expression, which promotes the SMC “contractile” phenotype and inhibits conversion to the “migratory/proliferative” phenotype.^{35,36}

Using rescue expression of Drebrin in SMCs *in vitro*, we showed directly that Drebrin suppresses the migratory/proliferative SMC phenotype. From our vascular remodeling experiments *in vivo*, we can also infer that the migratory/proliferative SMC phenotype is *promoted* by Drebrin *deficiency*: carotid de-endothelialization produced not only greater neointimal hyperplasia but also greater arterial expansion in *Dbn*^{-/+} mice. This arterial expansion, or “outward remodeling”, fundamentally involves the activity of matrix metalloproteinases secreted by activated SMCs.³⁷ Matrix metalloproteinase expression, in turn, upregulates when MRTF nuclear activity is reduced,³⁸ as would be expected in Drebrin-deficient SMCs, which have less F-actin, as we have shown.

Because Drebrin binds to Homer, which regulates TRP channels,¹⁶ it may seem surprising that Drebrin-dependent SMC TRP channel regulation does not involve Homer. However, TRP channel activity has been shown in other cells to be regulated by cytoskeletal reorganization.^{39,40} For example, the cell surface density of TRP channels in neutrophils is reduced by calyculin A, a phosphatase inhibitor which induces condensation of actin filaments at the plasma membrane; moreover, this effect is blocked by cytochalasin D, which inhibits actin polymerization.³⁹ In addition, Drebrin could reduce TRP channel activity by inhibiting the activity of α -actinin,³⁰ an actin-binding protein that can enhance TRP channel activity.⁴¹ Although Drebrin reduces SMC TRP channel activity, the molecular identity of the Drebrin-regulated SMC TRP channel(s) remains obscure, because SMCs express multiple TRP channels.^{24,42} We did not explore this issue, because disruption of a Homer-Drebrin interaction and pharmacologic inhibition of TRP channel activity had no effect on SMC migration in our assays. That pharmacologic inhibition of TRP channel activity had no effect on SMC migration in our assays may seem surprising in light of data implicating TRP channels in the regulation of vascular remodeling.¹³⁻¹⁵ The difference between our findings and previous studies¹³⁻¹⁵ may be due to differences in cell type or the fact the pharmacologic inhibition was used in the present work and gene silencing was used in previous studies. TRP channel knockdown would be expected to result in changes of expression of certain calcium-dependent signaling proteins or TRP channel interacting partners,^{43,44} whereas acute pharmacologic TRP channel inhibition over a shorter time period would not. In our studies, neither pharmacologic TRP channel inhibition nor disruption of the Homer-Drebrin interaction influenced the effects of Drebrin on SMC migration, indicating that Drebrin regulates SMC migration through its direct effect on actin filaments. While gadolinium is a non-selective channel blocker that also inhibits store-operated channels,⁴⁵ we observed no difference in store-operated currents in WT and *Dbn*^{-/+} SMCs to suggest a role for dysregulation of store-operated calcium influx in the phenotype of *Dbn*^{-/+} SMCs.

Because medial SMC Drebrin was upregulated in atherosclerotic lesions of mice and humans, it is conceivable that Drebrin activity reduces not only neointimal hyperplasia evoked by endothelial denudation but also atherogenesis. Arterial neointimal hyperplasia results from acute and chronic inflammatory signaling processes.²³ Consequently, gene products that affect neointimal hyperplasia in the absence of hyperlipidemia most often affect atherosclerosis in a concordant manner.^{22,23,46,47} Furthermore, gene products expressed solely in SMCs have been shown to affect atherosclerosis.^{46,47} Thus, although it is

expressed in SMCs but not in other cells involved in atherogenesis, Drebrin may prove to exert anti-atherogenic activity.

Supplementary Material

Refer to Web version on PubMed Central for supplementary material.

Acknowledgements

We would like to acknowledge Dr. Mary Hutson and the Duke Cardiovascular Research Center histology and microscopy core lab for technical assistance.

Sources of Funding

This work was supported by an American Heart Association Beginning Grant-in-Aid (J.A.S.); the Edna and Fred L. Mandel Jr. Foundation (J.A.S. and N.J.F.); NIH grants HL112901 (J.A.S and N.J.F.), HL121531 (J.A.S. and N.J.F.), AG028716 (J.A.S), and DK096493 (N.J.F.).

Nonstandard Abbreviations and Acronyms

Akt	protein kinase B
F-actin	filamentous actin
G-actin	globular actin
PDGF	platelet-derived growth factor
SM α-actin	smooth muscle α -actin
SMC	vascular smooth muscle cell
SM-MHC	smooth muscle myosin heavy chain
TRP	transient receptor potential

References

1. Shirao T, Kojima N, Kato Y, Obata K. Molecular cloning of a cDNA for the developmentally regulated brain protein, Drebrin. *Brain Res.* 1988; 464:71–74. [PubMed: 3179746]
2. Ishikawa R, Hayashi K, Shirao T, Xue Y, Takagi T, Sasaki Y, Kohama K. Drebrin, a development-associated brain protein from rat embryo, causes the dissociation of tropomyosin from actin filaments. *J Biol Chem.* 1994; 269:29928–29933. [PubMed: 7961990]
3. Geraldo S, Khanzada UK, Parsons M, Chilton JK, Gordon-Weeks PR. Targeting of the F-actin-binding protein Drebrin by the microtubule plus-tip protein EB3 is required for neuritogenesis. *Nat Cell Biol.* 2008; 10:1181–1189. [PubMed: 18806788]
4. Worth DC, Daly CN, Geraldo S, Oozeer F, Gordon-Weeks PR. Drebrin contains a cryptic F-actin-bundling activity regulated by CDK5 phosphorylation. *J Cell Biol.* 2013; 202:793–806. [PubMed: 23979715]
5. Kojima N, Shirao T, Obata K. Molecular cloning of a developmentally regulated brain protein, chicken Drebrin A and its expression by alternative splicing of the Drebrin gene. *Brain Res Mol Brain Res.* 1993; 19:101–114. [PubMed: 8361332]
6. Aoki C, Kojima N, Sabaliauskas N, Shah L, Ahmed TH, Oakford J, Ahmed T, Yamazaki H, Hanamura K, Shirao T. Drebrin A knockout eliminates the rapid form of homeostatic synaptic plasticity at excitatory synapses of intact adult cerebral cortex. *J Comp Neurol.* 2009; 517:105–121. [PubMed: 19711416]

7. Kojima N, Hanamura K, Yamazaki H, Ikeda T, Itohara S, Shirao T. Genetic disruption of the alternative splicing of Drebrin gene impairs context-dependent fear learning in adulthood. *Neuroscience*. 2010; 165:138–150. [PubMed: 19837137]
8. Jung G, Kim EJ, Cicvaric A, Sase S, Groger M, Hoger H, Sialana FJ, Berger J, Monje FJ, Lubec G. Drebrin depletion alters neurotransmitter receptor levels in protein complexes, dendritic spine morphogenesis and memory-related synaptic plasticity in the mouse hippocampus. *J Neurochem*. 2015; 134:327–339. [PubMed: 25865831]
9. Chew CS, Okamoto CT, Chen X, Thomas R. Drebrin E2 is differentially expressed and phosphorylated in parietal cells in the gastric mucosa. *American Journal of Physiology - Gastrointestinal & Liver Physiology*. 2005; 289:G320–331. [PubMed: 15790763]
10. Keon BH, Jedrzejewski PT, Paul DL, Goodenough DA. Isoform specific expression of the neuronal F-actin binding protein, Drebrin, in specialized cells of stomach and kidney epithelia. *J Cell Sci*. 2000; 113(Pt 2):325–336. [PubMed: 10633083]
11. Peitsch WK, Hofmann I, Endlich N, Pratzel S, Kuhn C, Spring H, Grone HJ, Kriz W, Franke WW. Cell biological and biochemical characterization of Drebrin complexes in mesangial cells and podocytes of renal glomeruli. *J Am Soc Nephrol*. 2003; 14:1452–1463. [PubMed: 12761245]
12. Goel M, Sinkins W, Keightley A, Kinter M, Schilling WP. Proteomic analysis of TRPC5- and TRPC6-binding partners reveals interaction with the plasmalemmal Na(+)/K(+)-ATPase. *Pflugers Arch*. 2005; 451:87–98. [PubMed: 16025302]
13. Golovina VA, Platoshyn O, Bailey CL, Wang J, Limsuwan A, Sweeney M, Rubin LJ, Yuan JX. Upregulated TRP and enhanced capacitative Ca(2+) entry in human pulmonary artery myocytes during proliferation. *Am J Physiol Heart Circ Physiol*. 2001; 280:H746–755. [PubMed: 11158974]
14. Berra-Romani R, Mazzocco-Spezia A, Pulina MV, Golovina VA. Ca2+ handling is altered when arterial myocytes progress from a contractile to a proliferative phenotype in culture. *Am J Physiol Cell Physiol*. 2008; 295:C779–790. [PubMed: 18596214]
15. Kumar B, Dreja K, Shah SS. *Circ Res*. 2006; 98:557–563. [PubMed: 16439693]
16. Yuan JP, Kiselyov K, Shin DM, Chen J, Shcheynikov N, Kang SH, Dehoff MH, Schwarz MK, Seeburg PH, Muallem S, Worley PF. Homer binds TRPC family channels and is required for gating of TRPC1 by IP3 receptors. *Cell*. 2003; 114:777–789. [PubMed: 14505576]
17. Stiber JA, Zhang ZS, Burch J, Eu JP, Zhang S, Truskey GA, Seth M, Yamaguchi N, Meissner G, Shah R, Worley PF, Williams RS, Rosenberg PB. Mice lacking Homer 1 exhibit a skeletal myopathy characterized by abnormal transient receptor potential channel activity. *Mol Cell Biol*. 2008; 28:2637–2647. [PubMed: 18268005]
18. Nepliouev I, Zhang ZS, Stiber JA. Effect of oxidative stress on Homer scaffolding proteins. *PLoS One*. 2011; 6:e26128. [PubMed: 22043307]
19. Shiraishi-Yamaguchi Y, Sato Y, Sakai R, Mizutani A, Knopfel T, Mori N, Mikoshiba K, Furuichi T. Interaction of Cupidin/Homer2 with two actin cytoskeletal regulators, CDC42 small GTPase and Drebrin, in dendritic spines. *BMC Neurosci*. 2009; 10:25. [PubMed: 19309525]
20. Mizutani A, Kuroda Y, Futatsugi A, Furuichi T. *J Neurosci*. 2008; 28:5369–5382. [PubMed: 18480293]
21. Shirao T, Kojima N, Terada S, Obata K. Expression of three Drebrin isoforms in the developing nervous system. *Neurosci Res Suppl*. 1990; 13:S106–111. [PubMed: 2259478]
22. Wu JH, Zhang L, Fanaroff AC, Cai X, Sharma KC, Brian L, Exum ST, Shenoy SK, Poppel K, Freedman NJ. G protein-coupled receptor kinase-5 attenuates atherosclerosis by regulating receptor tyrosine kinases and 7-transmembrane receptors. *Arterioscler Thromb Vasc Biol*. 2012; 32:308–316. [PubMed: 22095977]
23. Kim J, Zhang L, Poppel K, Wu JH, Zidar DA, Brian L, DeWire SM, Exum ST, Lefkowitz RJ, Freedman NJ. Beta-arrestins regulate atherosclerosis and neointimal hyperplasia by controlling smooth muscle cell proliferation and migration. *Circ Res*. 2008; 103:70–79. [PubMed: 18519945]
24. Bergdahl A, Gomez MF, Wihlborg AK, Erlinge D, Eyjolfson A, Xu SZ, Beech DJ, Dreja K, Hellstrand P. Plasticity of TRPC expression in arterial smooth muscle: Correlation with store-operated Ca2+ entry. *Am J Physiol Cell Physiol*. 2005; 288:C872–880. [PubMed: 15561760]
25. Trebak M, Bird GS, McKay RR, Putney JW Jr. Comparison of human TRPC3 channels in receptor-activated and store-operated modes. Differential sensitivity to channel blockers suggests

- fundamental differences in channel composition. *J Biol Chem.* 2002; 277:21617–21623. [PubMed: 11943785]
26. Potier M, Gonzalez JC, Motiani RK, Abdullaev IF, Bisaillon JM, Singer HA, Trebak M. Evidence for STIM1- and Orai1-dependent store-operated calcium influx through ICRAC in vascular smooth muscle cells: Role in proliferation and migration. *FASEB Journal.* 2009; 23:2425–2437. [PubMed: 19364762]
 27. Mancarella S, Potireddy S, Wang Y, Gao H, Gandhirajan RK, Autieri M, Scalia R, Cheng Z, Wang H, Madesh M, Houser SR, Gill DL. Targeted STIM deletion impairs calcium homeostasis, NFAT activation, and growth of smooth muscle. *FASEB J.* 2013; 27:893–906. [PubMed: 23159931]
 28. Mikati MA, Grintsevich EE, Reisler E. Drebrin-induced stabilization of actin filaments. *J Biol Chem.* 2013; 288:19926–19938. [PubMed: 23696644]
 29. Sharma S, Grintsevich EE, Phillips ML, Reisler E, Gimzewski JK. Atomic force microscopy reveals Drebrin induced remodeling of F-actin with subnanometer resolution. *Nano Lett.* 2011; 11:825–827. [PubMed: 21175132]
 30. Dun XP, Chilton JK. Control of cell shape and plasticity during development and disease by the actin-binding protein Drebrin. *Histol Histopathol.* 2010; 25:533–540. [PubMed: 20183806]
 31. Perez-Martinez M, Gordon-Alonso M, Cabrero JR, et al. F-actin-binding protein Drebrin regulates CXCR4 recruitment to the immune synapse. *J Cell Sci.* 2010; 123:1160–1170. [PubMed: 20215400]
 32. Boateng LR, Cortesio CL, Huttenlocher A. Src-mediated phosphorylation of mammalian ABP1 (DBNL) regulates podosome rosette formation in transformed fibroblasts. *J Cell Sci.* 2012; 125:1329–1341. [PubMed: 22303001]
 33. Collazo J, Zhu B, Larkin S, Martin SK, Pu H, Horbinski C, Koochekpour S, Kyprianou N. Cofilin drives cell-invasive and metastatic responses to TGF-beta in prostate cancer. *Cancer Res.* 2014; 74:2362–2373. [PubMed: 24509905]
 34. Grintsevich EE, Reisler E. Drebrin inhibits Cofilin-induced severing of F-actin. *Cytoskeleton (Hoboken).* 2014; 71:472–483. [PubMed: 25047716]
 35. Kuwahara K, Barrientos T, Pipes GC, Li S, Olson EN. Muscle-specific signaling mechanism that links actin dynamics to serum response factor. *Mol Cell Biol.* 2005; 25:3173–3181. [PubMed: 15798203]
 36. Li S, Wang DZ, Wang Z, Richardson JA, Olson EN. The serum response factor coactivator Myocardin is required for vascular smooth muscle development. *Proc Natl Acad Sci U S A.* 2003; 100:9366–9370. [PubMed: 12867591]
 37. Alexander MR, Moehle CW, Johnson JL, Yang Z, Lee JK, Jackson CL, Owens GK. Genetic inactivation of IL-1 signaling enhances atherosclerotic plaque instability and reduces outward vessel remodeling in advanced atherosclerosis in mice. *J Clin Invest.* 2012; 122:70–79. [PubMed: 22201681]
 38. Howard EW, Crider BJ, Updike DL, Bullen EC, Parks EE, Haaksma CJ, Sherry DM, Tomasek JJ. MMP-2 expression by fibroblasts is suppressed by the myofibroblast phenotype. *Exp Cell Res.* 2012; 318:1544–1553.
 39. Itagaki K, Kannan KB, Singh BB, Hauser CJ. Cytoskeletal reorganization internalizes multiple transient receptor potential channels and blocks calcium entry into human neutrophils. *J Immunol.* 2004; 172:601–607. [PubMed: 14688372]
 40. Redondo PC, Harper AG, Sage SO, Rosado JA. Dual role of tubulin-cytoskeleton in store-operated calcium entry in human platelets. *Cell Signal.* 2007; 19:2147–2154. [PubMed: 17681754]
 41. Li Q, Dai XQ, Shen PY, Wu Y, Long W, Chen CX, Hussain Z, Wang S, Chen XZ. Direct binding of alpha-actinin enhances TRPP3 channel activity. *J Neurochem.* 2007; 103:2391–2400. [PubMed: 17944866]
 42. Gonzalez-Cobos JC, Trebak M. TRPC channels in smooth muscle cells. *Front Biosci.* 2010; 15:1023–1039.
 43. Tajeddine N, Gailly P. TRPC1 protein channel is major regulator of epidermal growth factor receptor signaling. *J Biol Chem.* 2012; 287:16146–16157. [PubMed: 22451676]

44. Ong HL, Jang SI, Ambudkar IS. Distinct contributions of Orai 1 and TRPC1 to agonist-induced $[Ca^{2+}]_i$ signals determine specificity of Ca^{2+} -dependent gene expression. *PLoS One*. 2012; 7:e47146. [PubMed: 23115638]
45. Stiber J, Hawkins A, Zhang ZS, Wang S, Burch J, Graham V, Ward CC, Seth M, Finch E, Malouf N, Williams RS, Eu JP, Rosenberg P. STIM1 signalling controls store-operated calcium entry required for development and contractile function in skeletal muscle. *Nature Cell Biology*. 2008; 10:688–697. [PubMed: 18488020]
46. Boucher P, Gotthardt M, Li WP, Anderson RG, Herz J. LRP: Role in vascular wall integrity and protection from atherosclerosis. *Science*. 2003; 300:329–332. [PubMed: 12690199]
47. Subramanian V, Golledge J, Ijaz T, Bruemmer D, Daugherty A. Pioglitazone-induced reductions in atherosclerosis occur via smooth muscle cell-specific interaction with PPARgamma. *Circ Res*. 2010; 107:953–958. [PubMed: 20798360]

Significance

We found that expression of the actin-binding protein Drebrin is upregulated in atherosclerosis and in response to endothelial injury. Using a Drebrin loss of function model, we show that Drebrin is abundantly expressed in vascular smooth muscle cells and that Drebrin plays a critical function in smooth muscle cell migration and proliferation *in vitro* and *in vivo*. Furthermore, Drebrin regulates smooth muscle cell migration through its actin-stabilizing, rather than its Homer-binding activity. These data provide the first evidence that Drebrin stabilization of actin filaments plays a regulatory role in vascular remodeling.

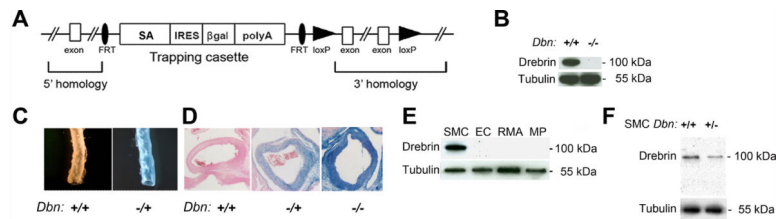


Figure 1. Drebrin gene trap reveals Drebrin expression in SMCs

A, Design of the *Dbn* targeting construct used to generate Drebrin KO mice. SA, splice acceptor; IRES, internal ribosome entry site; β gal, β -galactosidase gene; polyA, polyadenylation sequence; FRT, Flp recombinase target. **B**, Brain lysates from WT and *Dbn*^{-/-} neonatal mice were subjected to sequential immunoblotting for Drebrin and then tubulin, as indicated. **C-D**, Aortas from 8-wk-old mice of the indicated genotype were subjected to X-gal staining and (C) photographed at 5 \times magnification or (D) paraffin-embedded, sectioned, and counterstained with eosin. **E**, The following mouse cells were solubilized, and 30 μ g of cell protein was subjected to serial immunoblotting for Drebrin and tubulin: primary SMCs, primary endothelial cells (EC), RMA lymphoma cells (RMA), and primary macrophages (MP). **F**, Thirty μ g of protein from WT or *Dbn*^{+/-} SMCs were immunoblotted sequentially for Drebrin and then tubulin.

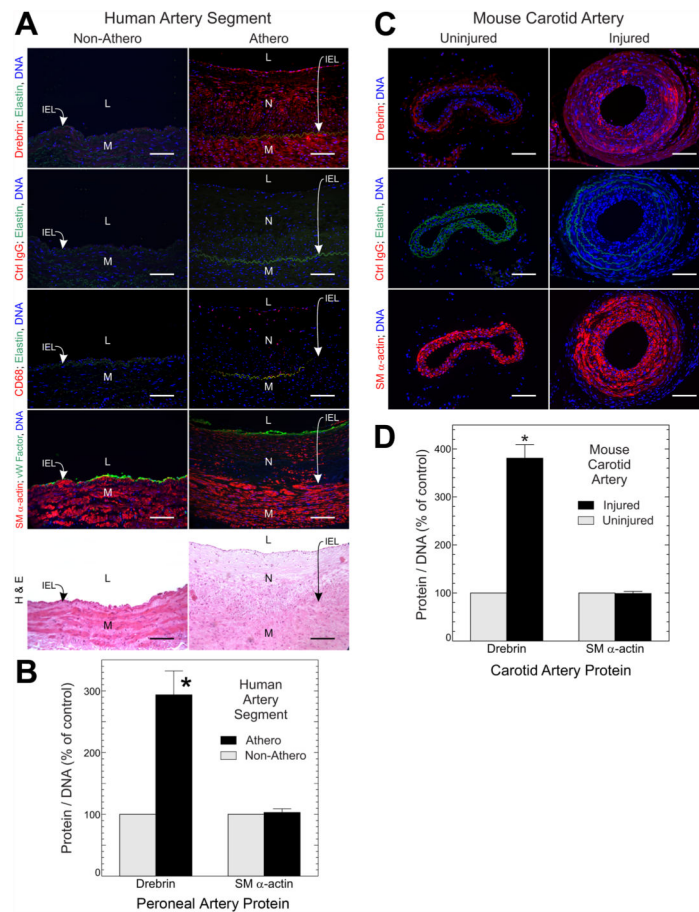


Figure 2. Debrin upregulates with atherosclerosis and arterial injury

A, Human peroneal arteries from surgically amputated legs were separated into segments that demonstrated atherosclerosis (“athero”) and segments with minimal or no atherosclerosis. Serial sections of these segments were immunostained for the indicated protein(s) (or with isotype control IgG), and counterstained with Hoechst 33342 (blue, DNA), or stained with hematoxylin and eosin (H&E). (Elastin autofluorescence is included to facilitate identification of the medial/neointimal boundary.) Letters designate the lumen (L), neointima (N), internal elastic lamina (IEL), and media (M); vWF = von Willebrand factor (in endothelial cells). Samples from a single staining session are shown, and represent 9 independent samples with equivalent results. The athero specimen (right) has pathological neointimal thickening (“subject 1,” Figure II of the online-only Data Supplement). Scale bar = 50 μ m. **B**, Drebrin and SM α -actin immunofluorescence intensities in the arterial media were normalized to corresponding DNA fluorescence intensities; the resulting ratios in each group were divided by cognate ratios obtained for “non-athero” control specimens, to obtain “% of control,” plotted as the means \pm SE from 9 specimens of each group. Compared with control: *, $p < 0.05$. **C**, Injured and contralateral uninjured (“control”) mouse carotid arteries were sectioned serially and immunostained with anti-Drebrin IgG, isotype control IgG, or anti-SM α -actin IgG, as indicated, and counterstained with Hoechst 33342 (blue, DNA). Samples from a single staining session are shown, and represent 4 independent samples with equivalent results. Scale bar = 100 μ m. **D**, Drebrin and SM α -actin immunofluorescence in

the arterial media were normalized to DNA fluorescence; these ratios are plotted (“arbitrary units”) as the means \pm SE from 4 independent carotid arteries. Compared with control: *, $p < 0.01$.

Author Manuscript

Author Manuscript

Author Manuscript

Author Manuscript

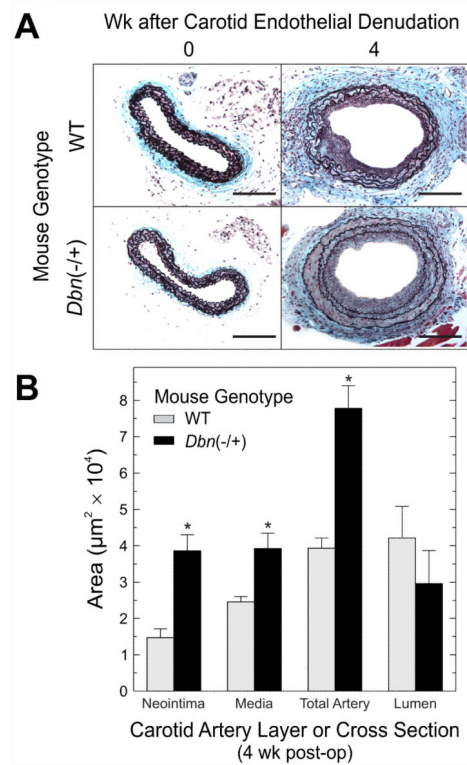


Figure 3. Drebrin reduces neointimal hyperplasia

A, WT (n=8) and congenic *Dbn*^{-/+} mice (n=5) were subjected to wire-mediated carotid endothelial denudation and sacrificed 4 wk later. Injured and contralateral control (“0” wk post-injury) carotids were sectioned and stained with a modified connective tissue stain. Scale bar = 100 μm . **B**, The indicated cross-sectional areas were quantitated by computerized planimetry (see Methods), and plotted as means \pm SE from 5 specimens of each genotype. Compared with WT: *, $p < 0.01$.

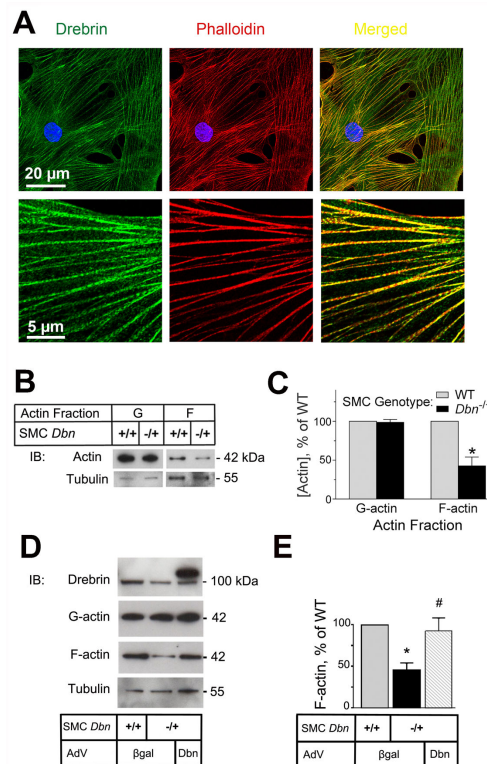


Figure 4. Drebrin stabilizes actin filaments in SMCs

A, Primary mouse SMCs were fixed and stained with both rabbit anti-Drebrin IgG (green) and Alexa-555-phalloidin (red, for F-actin), and then imaged by confocal microscopy in the identical z-plane with post-acquisition merging of red and green channels (right). Shown are images from a single SMC, representative of hundreds of SMCs imaged in four independent staining sessions. **B**, Lysates from SMCs of the indicated genotypes were subjected to actin fractionation by ultracentrifugation, as in Methods. The supernatant (G-actin) and pellet (F-actin) were immunoblotted serially for β -actin and then tubulin. Shown are results from a single experiment, representative of 3 performed with independent WT and cognate *Dbn*^{-/+} SMC lines. **C**, Band densities for G- and F-actin were normalized to cognate tubulin band densities; within each experiment these quotients were divided by that obtained for WT SMCs, to obtain “% of WT”, plotted as means \pm SE from 3 experiments. Compared with WT: *, $p < 0.05$. **D**, WT and *Dbn*^{-/+} SMCs were transduced with either control (β gal) or Drebrin-encoding (Dbn) adenovirus: subsequently actin in SMC lysates was fractionated and immunoblotted as in panel B. Shown are results from a single experiment, representative of 3 performed with independent WT and cognate *Dbn*^{-/+} SMC lines. **E**, Band density data for F-actin was processed as in panel C, and plotted as means \pm SE from 3 experiments. Compared with WT: *, $p < 0.05$. Compared with cognate β -gal transduced SMCs: #, $p < 0.05$.

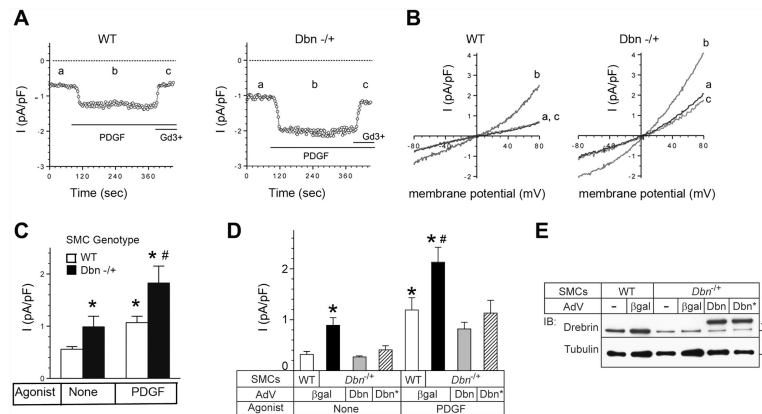


Figure 5. Loss of Drebrin results in increased TRP channel activity

A, WT and cognate *Dbn*^{-/-} SMCs were subjected to whole-cell patch clamping as in Methods, and stimulated with 1 nmol/L PDGF-BB for the indicated time. Current induced as in Methods was plotted vs time for the indicated SMCs under basal conditions (a), after stimulation with 1 nmol/L PDGF (b), and after addition of 10 μmol/L Gd³⁺ (c). Shown are inward current tracings from a single experiment, representative of 18 WT and 14 *Dbn*^{-/-} SMCs respectively. **B**, Representative tracings showing current-voltage relationships for the indicated SMCs under basal conditions (a), after stimulation with 1 nmol/L PDGF (b), and after addition of 10 μmol/L Gd³⁺ (c). Shown are current-voltage relationships from a single experiment, representative of the same numbers of SMCs of each genotype as in A. **C**, The mean inward current density at a potential of -80 mV was measured before and after 1 nmol/L PDGF-BB for WT (n=18) and *Dbn*^{-/-} (n=14) SMCs, and plotted as means ± SE. Compared with WT unstimulated: *, p < 0.05. Compared with PDGF-stimulated WT: #, p < 0.05. SMCs used for measurements of TRP current density were obtained from four independent WT and cognate *Dbn*^{-/-} SMC lines. **D**, WT and *Dbn*^{-/-} SMCs were transduced with recombinant adenoviruses encoding β-galactosidase (βgal), Drebrin (Dbn), or a Drebrin mutant (F543A/F621A, Dbn*) that cannot bind Homer. Inward current density was measured as in panel C, for WT SMCs transduced with βgal (n=7) or *Dbn*^{-/-} SMCs transduced with βgal (n=9), Dbn (n=8) or Dbn* (n=9). Results are plotted as means ± SE. Compared with WT unstimulated: *, p < 0.05. Compared with PDGF-stimulated WT: #, p < 0.05. **E**, WT and *Dbn*^{-/-} SMCs from panel D were solubilized and subjected to SDS/PAGE followed by serial immunoblotting (IB) for Drebrin and tubulin.

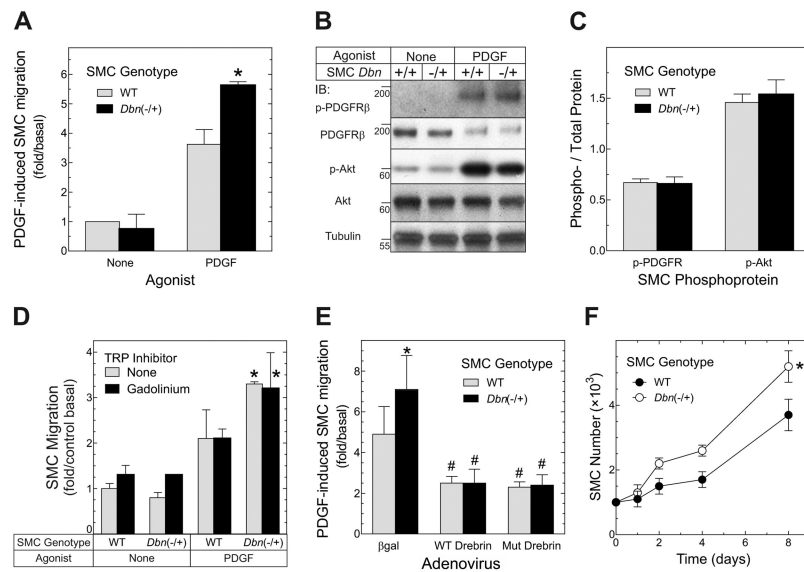


Figure 6. Drebrin inhibits SMC migration and proliferation

A, *Dbn*^{-/-} and WT SMCs in a modified Boyden chamber were challenged ±PDGF-BB (0.4 nmol/L) in serum-free medium, and migrated SMCs were quantitated as in Methods. The number of migrated SMCs was normalized to that obtained for unstimulated WT SMCs, to obtain “fold/basal,” plotted as means ± SE of 3 experiments performed with independent WT and *Dbn*^{-/-} SMCs. Compared with WT: *, *p* < 0.05. **B**, Quiescent WT and *Dbn*^{-/-} SMCs were challenged ±PDGF-BB (0.4 nmol/L) for 15 min (37 °C), and then solubilized; extracts were immunoblotted serially for phospho- (“p”) PDGFRβ (Y857) (PDGFRβ autophosphorylated on its key activation loop Tyr857), total PDGFRβ, p-Akt(Ser473), total Akt, and tubulin. Results are from a single experiment, representative of 3 performed. **C**, The band densities for the indicated phosphoprotein were normalized to the densities of cognate “total” protein bands from panel **B**, and plotted as the means ± SE of 3 independent experiments performed with 3 independently isolated SMC lines of each genotype. **D**, *Dbn*^{-/-} and WT SMCs were subjected to migration assays as in **A**, but in the absence or presence of the TRP channel inhibitor gadolinium (10 μmol/L GdCl₃). The number of SMCs migrated were normalized to the number obtained with WT SMCs in the absence of stimulus or GdCl₃, to obtain “fold/control basal”, plotted as means ± SE from 3 independent experiments. Compared with WT: *, *p* < 0.05. **E**, *Dbn*^{-/-} and WT SMCs were transduced with recombinant adenoviruses encoding β-galactosidase (“βgal”), WT Drebrin, or the F543A/F621A mutant (“Mut”) Drebrin that cannot bind to Homer; these SMCs were then subjected to migration assays as in **A** and **C**. The number of SMCs migrated in response to PDGF was normalized to that obtained with unstimulated SMCs to obtain “fold/basal”, plotted as means ± SE of 3 independent experiments performed with 3 independent lines of *Dbn*^{-/-} and WT SMCs. Compared with WT: *, *p* < 0.05. Compared with cognate βgal-transduced SMCs: #, *p* < 0.05. **F**, *Dbn*^{-/-} and WT SMCs were subjected to proliferation assays in the presence of 10% FBS, as described in Methods. Plotted are the means ± SE of 3 independent experiments performed with 3 independent lines of *Dbn*^{-/-} and WT SMCs. Compared with the WT SMC growth curve: *, *p* < 0.05.

Table 1

Dbn^{-/+} mice were mated to generate *Dbn*^{-/-} mice, which were initially viable but died prior to weaning (P21) ($X^2 = 16.7$, 2 degrees of freedom, $p = 0.001$). The number of offspring for each genotype is indicated for observed and expected numbers (parentheses) based on Mendelian ratios of 1:2:1 on embryonic day 14.5 (E14.5), the day of birth (P0-1), and the day of weaning (P21). Subsequent genotyping analysis revealed neonatal mortality within 48 hours of birth.

Analysis of Offspring of Intercrossed Heterozygotes						
Age	WT	Het	KO	Total	X^2	p
E14.5	5 (4.25)	5 (8.5)	7 (4.25)	17	1.64	NS
P0-1	11 (8.75)	13 (17.5)	11 (8.75)	35	1.18	NS
P21	28 (19.5)	48 (39)	2 (19.5)	78	16.7	0.001